Output feedback sliding mode control for the flying height of a pickup head in near-field optical disk drives

W.C. Wu and T.S. Liu

Abstract: An output sliding mode control method to produce a stable flying height for a pickup head in a near-field optical disk drive is presented. When the optical disks have a large amplitude vibration that makes a stable flying height difficult to attain, a piezoelectric bender is used to complement an air bearing at the head/disk interface. Control simulation for an identified model using measured vibration data of an optical disk is performed to demonstrate the robustness of the proposed method.

1 Introduction

Optical disks are popular due to their large data storage capacity, and as such they find extensive use in audio and video media. The need for a large data storage capacity and high quality recording media has resulted in high data storage density requirements for optical disks [1, 2]. However, due to light wave diffraction in a far-field optical environment, the optical pickup device cannot further reduce the light spot size to access a smaller data track width and thereby accomplish a higher data recording density. The application of near-field optics to avoid the diffraction limitation requires the near-field optical disk drives to adopt the structure of a magnetic disk drive but with the magnetic pickup being replaced by a near-field optical pickup head. This allows the disk drive to maintain the space between the pickup head and disk within the near-field focusing length. Thus, the recording density can be increased by means of an improvement in the optical resolution. Additionally, optical disks are generally made out of a plastic-based material due to its low cost. Hence, the optical disk vibration magnitude will be larger than that in an aluminum-substrate hard disk. Therefore, the passive air bearing flying height mechanism barely attains the focusing performance requirement in the presence of severe disk vibration. In order to circumvent the problem and achieve a satisfactory performance in flying height control, we attach a multi-layer piezoelectric bender (PZT) to the suspension arm to serve as an active flying height controller. Similar designs have been widely used in hard disk drives to achieve head-disk spacing control and fine track following control [3, 4].

We aim to apply an output feedback sliding mode controller for flying height control by using a PZT bender. The sliding mode control method is popular due to its properties of robustness and insensitivity to matched disturbance and model uncertainty [5, 6]. Conventional sliding mode control is based on a state-space design, where information on the system states is needed when constructing the sliding surface and controller. However, system states are not measurable in the current study; hence, an output feedback sliding mode control method that solely uses the output error is developed. An output feedback sliding mode controller is developed first to validate the performance of the flying height control. The first and second derivatives of the flying height error are needed in the controller. However, this may result in difficulties in practice due to measurement noise. Therefore, a high-order sliding mode control method [7] with robust differentiators [8] is used to reduce the number of required output derivatives and to avoid the influence of measurement noise. In addition, a high-order sliding mode controller helps to reduce chattering with appropriate order design [7, 9]. Simulations on an identified model using measured vibration data of an optical disk will be presented to demonstrate the controller effectiveness.

2 Flying height control mechanism

To enable the active flying height control capability, a modified flying head with a PZT actuator is fixed to a suspension arm, as shown in Fig. 1. The PZT serves as the flying height actuator for the flying head in a near-field optical disk drive. This approach has been used as a fine actuator in high density data storage disk drives, since its response performance is sufficient to achieve a fast and precise movement. With a laser Doppler vibrometer in the system identification, a PZT transfer function that relates the control voltage U in volts to the PZT bending displacement Y in nanometres in the vertical direction is:

$$\frac{Y(s)}{U(s)} = (3.188\times10^{15}(s^2+19.85s+1.096\times10^7))\Big/ ((s+2.545\times10^4)(s^2+141.2s+4.797\times10^6) \times (s^2+534.9s+1.068\times10^8)) \quad (1)$$

As a result, a Bode diagram and an open-loop step response are shown in Figs. 2 and 3, respectively. Considering the

IEE Proceedings online no. 20030885

doi: 10.1049/ip-cta:20030885

Paper first received 17th January 2003 and in revised form 8th July 2003

The authors are with Department of Mechanical Engineering, National Chiao Tung University, Hsinchu 30010, Taiwan, Republic of China

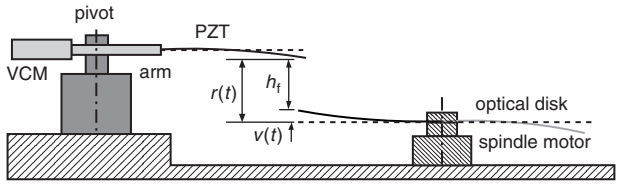

Fig. 1 *Flying head with an embedded PZT actuator*

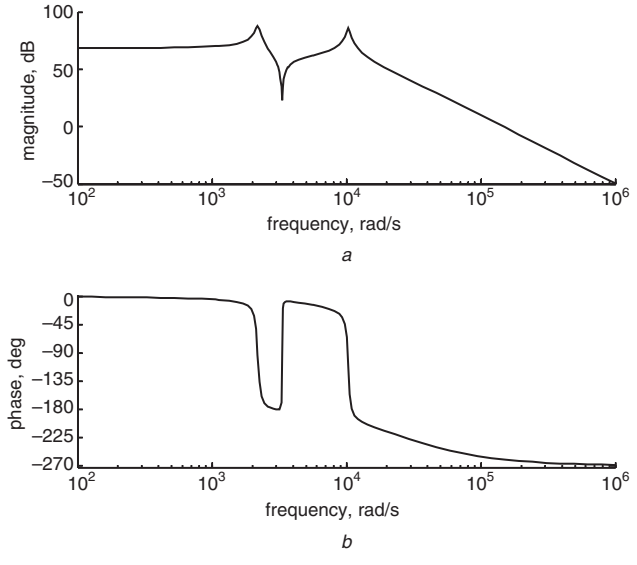

Fig. 2 *Bode diagram of open loop system*

a Magnitude as a function of frequency
b Phase as a function of frequency

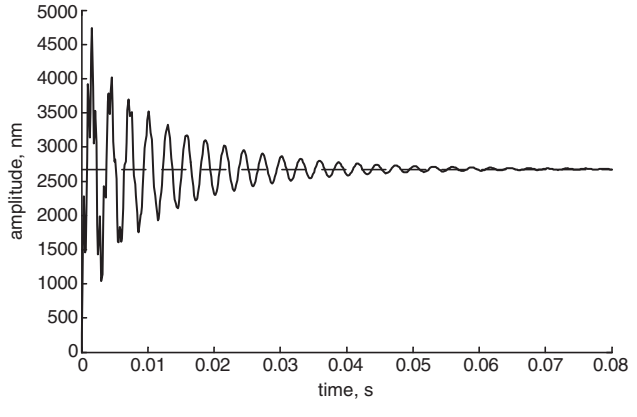

Fig. 3 *Step response of open-loop system*

open-loop step response shown in Fig. 3, there is an obvious oscillation in the transient response which results in a long settling time. Hence, a closed-loop controller is required to eliminate the flying height oscillation and obtain a fast and stable response.

3 Output feedback sliding mode control

The flying head is required to undergo a desired displacement, q_d, in the vertical direction in order to maintain a constant flying height between the vibratory optical disk and the optical flying head. The trajectory of the desired displacement q_d generally will be the optical disk vibration waveform plus a constant flying height. In view of uncertainties and disturbances in the current system, a sliding mode control method is applied.

The PZT plant model in (1) can be rewritten in state-variable form as:

$$\begin{aligned}\dot{\boldsymbol{x}} &= \boldsymbol{A}\boldsymbol{x} + \boldsymbol{B}u + \boldsymbol{d}(\boldsymbol{x},t)\\ &= \begin{bmatrix} a_1 & a_2 & a_3 & a_4 & a_5\\ 1 & 0 & 0 & 0 & 0\\ 0 & 1 & 0 & 0 & 0\\ 0 & 0 & 1 & 0 & 0\\ 0 & 0 & 0 & 1 & 0 \end{bmatrix}\begin{bmatrix} x_1\\ x_2\\ x_3\\ x_4\\ x_5 \end{bmatrix} + \begin{bmatrix} b_1\\ 0\\ 0\\ 0\\ 0 \end{bmatrix} u + \begin{bmatrix} d_1\\ d_2\\ d_3\\ d_4\\ d_5 \end{bmatrix}\\ y &= \boldsymbol{H}\boldsymbol{x}\\ &= [0 \quad 0 \quad h_3 \quad h_4 \quad h_5]\boldsymbol{x} \end{aligned} \tag{2}$$

where $y(t) \in \mathrm{R}$ is the flying height, $u(t) \in \mathrm{R}$ is the control input voltage, and the system state vector $\boldsymbol{x}(t) \in \mathrm{R}^5$. Additionally, the disturbance vector $\boldsymbol{d}(\boldsymbol{x},t) \in \mathrm{R}^5$ caused by system uncertainty and external noise is bounded by:

$$\|\boldsymbol{d}(\boldsymbol{x},t)\| \leq \delta(\boldsymbol{x},t) \tag{3}$$

and $\delta(\boldsymbol{x},t)$ is a known boundary function.

In near-field optical disk drives, the only feedback information about the flying head generally will be either the displacement or the velocity. Not all system states are available and we assume that only the output displacement error can be obtained. As a consequence, the control design method using system states can not be used and thus an output feedback sliding mode control will be developed.

The flying height error is defined as:

$$e = y - q_d \tag{4}$$

Since the relative degree of the system is three according to (1), the twice differentiation term $\ddot{e}$ is incorporated in the sliding surface design. Hence, a sliding surface $s(\boldsymbol{e})$ is prescribed in terms of error terms:

$$s(\boldsymbol{e}) = \boldsymbol{C}\boldsymbol{e} = [1 \quad \Lambda \quad \Gamma]\begin{bmatrix} \ddot{e}\\ \dot{e}\\ e \end{bmatrix} = \ddot{e} + \Lambda\dot{e} + \Gamma e \tag{5}$$

where coefficients Λ and Γ come from the sliding mode conjugate poles $p_1 = -\alpha + \beta j$ and $p_2 = -\alpha - \beta j$ as:

$$\boldsymbol{C} = [1 \quad \Lambda \quad \Gamma] = [1 \quad 2\alpha \quad \alpha^2 + \beta^2 + 2\alpha\beta] \tag{6}$$

As long as a sliding mode of the system trajectory exists on a sliding surface $s(\boldsymbol{e}) = 0$, a continuous control u_{eq} called 'equivalent control' [5] and [6] can replace the undefined discontinuous control on the discontinuity boundary to make the system trajectory continuous along the surface $s(\boldsymbol{e}) = 0$ [6]. Since the system trajectory in the sliding mode is continuous, the sliding function $s(\boldsymbol{e})$ represented in (5) must be differentiable. This means that the time derivative of $s(\boldsymbol{e})$ in (5) is equal to zero; i.e.:

$$\dot{s}(\boldsymbol{e})|_{u=u_{eq}} = e^{(3)} + \Lambda\ddot{e} + \Gamma\dot{e} = 0 \tag{7}$$

Assuming the desired displacement q_d is a constant and taking the triple differentiation of (4), leads to:

$$e^{(3)} = y^{(3)} - q_d^{(3)} = y^{(3)} \tag{8}$$

Substituting (8) into (7) yields:

$$\dot{s}(\boldsymbol{e})|_{u=u_{eq}} = y^{(3)} + \Lambda\ddot{e} + \Gamma\dot{e} = 0 \tag{9}$$

Further, substituting the state equation from (2) into (9) yields:

$$
\begin{aligned}
\dot{s}(\boldsymbol{e})|_{u=u_{eq}} &= \frac{d^3}{dt^3}(h_3x_3 + h_4x_4 + h_5x_5) + \Lambda\ddot{e} + \Gamma\dot{e} \\
&= \frac{d^2}{dt^2}(h_3x_2 + h_4x_3 + h_5x_4 + h_3d_3 + h_4d_4 + h_5d_5) \\
&\quad + \Lambda\ddot{e} + \Gamma\dot{e} \\
&= \frac{d}{dt}(h_3x_1 + h_4x_2 + h_5x_3 + h_3d_2 + h_4d_3 + h_5d_4 \\
&\quad + h_3d_3 + h_4d_4 + h_5d_5) + \Lambda\ddot{e} + \Gamma\dot{e} \\
&= h_3(a_1x_1 + a_2x_2 + a_3x_3 + a_4x_4 + a_5x_5 + u + d_1) \\
&\quad + h_4x_1 + h_5x_2 + h_4d_2 + h_5d_3 + h_3\dot{d}_2 \\
&\quad + (h_4 + h_3)\dot{d}_3 + (h_5 + h_4)\dot{d}_4 + h_5\dot{d}_5 + \Lambda\ddot{e} + \Gamma\dot{e} \\
&= 0
\end{aligned} \tag{10}
$$

It follows from (10) that the equivalent control u_{eq} can be written as:

$$
\begin{aligned}
u &= u_{eq} \\
&= -\left(a_1x_1 + a_2x_2 + a_3x_3 + a_4x_4 + a_5x_5 + \frac{h_4}{h_3}x_1 + \frac{h_5}{h_3}x_2\right) \\
&\quad - \frac{1}{h_3}d_f - \frac{\Lambda}{h_3}\ddot{e} - \frac{\Gamma}{h_3}\dot{e}
\end{aligned} \tag{11}
$$

where $d_f = h_3d_1 + h_4d_2 + h_5d_3 + h_3\dot{d}_2 + (h_4 + h_3)\dot{d}_3 + (h_5 + h_4)\dot{d}_4 + h_5\dot{d}_5$, and hence, it depends on the disturbance terms.

Sliding mode control has to enable a system to move towards and stay on a sliding surface; i.e. satisfy the reaching and sliding condition [6]:

$$
s\dot{s} < -\kappa|s| \tag{12}
$$

where κ is a positive constant, so that the system trajectory reaches the sliding surface in a finite time. Therefore, based on (11), for output feedback sliding mode control we define the control input u as:

$$
\begin{aligned}
u = & -\left(\left|a_1x_1 + a_2x_2 + a_3x_3 + a_4x_4 + a_5x_5 + \frac{h_4}{h_3}x_1\right.\right. \\
& \left.\left. + \frac{h_5}{h_3}x_2 + \frac{1}{h_3}d_f\right|_{max} + \kappa\right)\mathrm{sgn}(s) - \frac{\Lambda}{h_3}\ddot{e} - \frac{\Gamma}{h_3}\dot{e} \\
= & -(|f(\boldsymbol{x}) + kd_f|_{max} + \kappa)\mathrm{sgn}(s) - k\Lambda\ddot{e} - k\Gamma\dot{e} \\
= & -Q\,\mathrm{sgn}(s) - k\Lambda\ddot{e} - k\Gamma\dot{e}
\end{aligned} \tag{13}
$$

where

$$
\mathrm{sgn}(s) = \begin{cases} +1 & \text{if } s > 0 \\ 0 & \text{if } s = 0 \\ -1 & \text{if } s < 0 \end{cases} \tag{14}
$$

$$
\begin{aligned}
& f(\boldsymbol{x}) = a_1x_1 + a_2x_2 + a_3x_3 + a_4x_4 + a_5x_5 + \frac{h_4}{h_3}x_1 + \frac{h_5}{h_3}x_2, \\
& 1 > k = \frac{1}{h_3} > 0 \\
& Q = (|f(\boldsymbol{x}) + kd_f|_{max} + \kappa) > 0
\end{aligned} \tag{15}
$$

Proof: Substituting (10) and (13) into the reaching and sliding condition in (12) yields

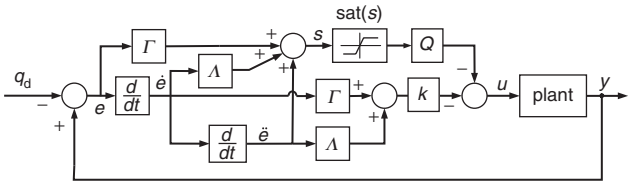

Fig. 4 *Block diagram of closed-loop sliding mode control system*

$$
\begin{aligned}
s\dot{s} &= s[h_3(a_1x_1 + a_2x_2 + a_3x_3 + a_4x_4 + a_5x_5 + u + h_1d_1) \\
&\quad + h_4x_1 + h_5x_2 + h_4d_1 + h_5d_2 + h_3\dot{d}_1 + h_4\dot{d}_2 + h_3\dot{d}_2 \\
&\quad + h_5\dot{d}_3 + h_4\dot{d}_3 + h_5\dot{d}_4 + \Lambda\ddot{e} + \Gamma\dot{e}] \\
&= s[h_3f(\boldsymbol{x}) + d_f + h_3u + \Lambda\ddot{e} + \Gamma\dot{e}] \\
&= s\left[h_3f(\boldsymbol{x}) + d_f - h_3\left(\left|f(\boldsymbol{x}) + \frac{1}{h_3}d_f\right|_{max} + \kappa\right)\mathrm{sgn}(s)\right] \\
&= h_3\left(f(\boldsymbol{x}) + \frac{1}{h_3}d_f\right)s - h_3\left|f(\boldsymbol{x}) + \frac{1}{h_3}d_f\right|_{max}|s| - h_3\kappa|s|
\end{aligned} \tag{16}
$$

However:

$$
\left(f(\boldsymbol{x}) + \frac{1}{h_3}d_f\right)s < \left|f(\boldsymbol{x}) + \frac{1}{h_3}d_f\right|_{max}|s|
$$

and from (15), one has $h_3 > 1$, hence, (16) yields $s\dot{s} < -\kappa|s|$. This proves the reaching and sliding condition in (12) for the proposed output feedback sliding mode controller. □

Since the control law given in (13) is discontinuous across the sliding surface, it gives rise to chattering in a trajectory tracking process. Therefore, a saturation function $\mathrm{sat}(s)$ with a sliding layer ε is adopted to replace the switching function $\mathrm{sgn}(s)$ defined in (14), i.e.:

$$
\mathrm{sat}(s) = \begin{cases} \mathrm{sgn}(s) & |s| > \varepsilon \\ \dfrac{s}{\varepsilon} & |s| \le \varepsilon \end{cases} \tag{17}
$$

The controller in (13) can thus be written as:

$$
u = -Q\,\mathrm{sat}(s) - k\Lambda\ddot{e} - k\Gamma\dot{e} \tag{18}
$$

The closed-loop block diagram with output feedback sliding mode control is shown in Fig. 4. Since the maximum boundary of the system states function $f(\boldsymbol{x})$ and disturbances $\delta(\boldsymbol{x}, t)$ is usually unknown or inaccurate. The design parameter Q in (18) can be adjusted based on an energy function expressed by:

$$
E(e) = \int e^2dt \tag{19}
$$

in order to minimise the control error.

4 Output feedback high-order sliding mode control

The sliding surface in (5) adopts $\ddot{e}$ and $\dot{e}$ in order to construct an output feedback sliding mode controller. Since only flying height error can be measured in practice, the first and second differentiation of e are used instead of direct measurements of $\dot{e}$ and $\ddot{e}$. Hence, a high-order sliding mode controller with robust differentiators is presented for the flying height control. Using high-order sliding mode reduces the number of output derivatives required and the robust differentiator yields exact differentiation with finite-time convergence.

4.1 Third-order sliding mode controller

Considering the system in (1) of relative degree three, a third-order sliding mode controller design is adopted. The control purpose is to eliminate the flying height error, hence, the sliding surface is defined as:

$$\sigma = e = y - q_d \tag{20}$$

With the sliding surface, a general form of relay type third-order sliding mode control for a relative degree three system can be written as [7]:

$$u = -A_3 \operatorname{sgn}\left[\ddot{\sigma} + 2\left(|\dot{\sigma}|^3 + \sigma^2\right)^{1/6} \operatorname{sgn}\left(\dot{\sigma} + |\sigma|^{2/3} \operatorname{sgn} \sigma\right)\right] \tag{21}$$

where A_3 is a positive constant. Accordingly, to use (21) only knowledge of the relative degree of the system is needed in advance while the exact plant model is not required. Thus, the information needed is simply the current value of σ. In (21), the required time derivatives of σ can be evaluated by various differentiators [10] and [11]. To modify (21), define sliding functions as [12]:

$$S_0 = \sigma \tag{22}$$

$$S_1 = \dot{S}_0 + A_1 |S_0|^{2/3} \operatorname{sgn}(S_0) \tag{23}$$

where A_1 is a positive constant. Using (22) and (23), then (21) becomes an output feedback third-order sliding mode controller expressed by:

$$u = -A_3 \operatorname{sgn}\{\dot{S}_1 + A_2 |S_1|^{1/6} \operatorname{sgn}[\dot{S}_0 + A_1 |S_0|^{2/3} \operatorname{sgn}(S_0)]\} \tag{24}$$

where A_2 is a positive constant. Further, (24) can be rewritten as:

$$u = -A_3 \operatorname{sgn}(S_2) \tag{25}$$

where

$$S_2 = \dot{S}_1 + A_2 |S_1|^{1/6} \operatorname{sgn}(S_1) \tag{26}$$

4.2 Robust differentiator

To implement the above controller in (24) we require information on the successive derivatives $\dot{S}_0$ and $\dot{S}_1$. Hence, a robust differentiator is adopted to evaluate exact derivative values. A general form of arbitrary order robust differentiator can be applied as [13]:

$$\begin{aligned}
\dot{z}_0 &= -\kappa_0 |z_0 - f(t)|^{n/(n+1)} \operatorname{sgn}(z_0 - f(t)) + z_1 \\
&\cdots \\
\dot{z}_i &= -\kappa_i |z_0 - f(t)|^{(n-i)/n+1} \operatorname{sgn}(z_0 - f(t)) + z_{i+1} \\
&\quad i = 1, \ldots, n-1 \\
\dot{z}_n &= -\kappa_n \operatorname{sgn}(z_0 - f(t))
\end{aligned} \tag{27}$$

where $z_0, z_1, \ldots, z_n$ are estimations of input $f(t), \dot{f}(t), \ldots, f^{(n)}(t)$ and $\kappa_0, \ldots, \kappa_n$ are positive constants. Using (27), the control input in (24) can be rewritten as:

$$u = -A_3 \operatorname{sgn}\left\{\nu_1 + A_2 |\nu_0|^{1/6} \operatorname{sgn}\left[\mu_1 + A_1 |\mu_0|^{2/3} \operatorname{sgn}(\mu_0)\right]\right\} \tag{28}$$

with the robust differentiators being written as:

$$\begin{aligned}
\dot{\mu}_0 &= -\bar{\kappa}_0 |\mu_0 - S_0|^{1/2} \operatorname{sgn}(\mu_0 - S_0) + \mu_1 \\
\dot{\mu}_1 &= -\bar{\kappa}_1 \operatorname{sgn}(\mu_0 - S_0)
\end{aligned} \tag{29}$$

and

$$\begin{aligned}
\dot{\nu}_0 &= -\tilde{\kappa}_0 |\nu_0 - S_1|^{1/2} \operatorname{sgn}(\nu_0 - S_1) + \nu_1 \\
\dot{\nu}_1 &= -\tilde{\kappa}_1 \operatorname{sgn}(\nu_0 - S_1)
\end{aligned} \tag{30}$$

where the value of the sliding function S_1 was evaluated by:

$$S_1 = \mu_1 + A_1 |\mu_0|^{2/3} \operatorname{sgn}(\mu_0) \tag{31}$$

4.3 Fourth-order sliding mode control

In order to eliminate chattering, it was proved by [7] that introducing successive time derivatives $u, \dot{u}, \ldots, u^{(r-k-1)}$ as new auxiliary variables and $u^{(r-k)}$ as a new control input achieves different modifications of each rth order sliding mode controller with a system relative degree of $k = 1, 2, \ldots, r$. The resulting control input is a $(r-k-1)$ smooth function of time when $k < r$, a Lipschitz function when $k = r-1$, and a bounded infinite-frequency switching function when $k = r$. Accordingly, in order to generate a control input that is smoother than an infinite-frequency switching one, a fourth-order sliding mode control is designed by modifying the original system in (2) as:

$$\begin{aligned}
\dot{\boldsymbol{x}} &= \boldsymbol{A}\boldsymbol{x} + \boldsymbol{B}u \\
y &= \boldsymbol{H}\boldsymbol{x} \\
\dot{u} &= \tau
\end{aligned} \tag{32}$$

where the actual control input u of the original system is treated as a new auxiliary variable of the higher relative degree system in (32) and τ is the new control input of the fourth-order sliding mode control written as:

$$\begin{aligned}
\tau &= -A_4 \operatorname{sgn}\langle \dot{S}_2 + A_3 |S_2|^{1/12} + \operatorname{sgn}\{\dot{S}_1 + A_2 |S_1|^{1/6} \\
&\quad \times \operatorname{sgn}[\dot{S}_0 + A_1 |S_0|^{2/3} \operatorname{sgn}(S_0)]\}\rangle \\
&= -A_4 \operatorname{sgn}(S_3)
\end{aligned} \tag{33}$$

where

$$\begin{aligned}
S_0 &= \sigma \\
S_1 &= \dot{S}_0 + A_1 |S_0|^{2/3} \operatorname{sgn}(S_0) \\
S_2 &= \dot{S}_1 + A_2 |S_1|^{1/6} \operatorname{sgn}(S_1) \\
S_3 &= \dot{S}_2 + A_3 |S_2|^{1/12} \operatorname{sgn}(S_2)
\end{aligned} \tag{34}$$

The robust differentiators in (27) can be applied here in a manner similar to Section 4.2 that deals with the third-order sliding mode controller.

5 Flying height control simulation

5.1 Output feedback sliding mode control

With the plant model in (1), Figs. 5*a* and 5*b* compare simulation results of the output feedback sliding mode controller with a switching function $\operatorname{sgn}(s)$ in (13) and a saturation function $\operatorname{sat}(s)$ in (18). The 1000 nm step responses and sliding surfaces are shown in Figs. 5*a* and 5*b*, respectively. It is demonstrated that the saturation function indeed eliminates chattering. Figures 6*a* and 6*b* respectively compare 10 nm step responses and control inputs with and without white noise in the control input. The mean and variance of the white noise are 0.0475 and 3.2526, respectively. As a result, the flying height is not affected, although the control input is accompanied by white noise.

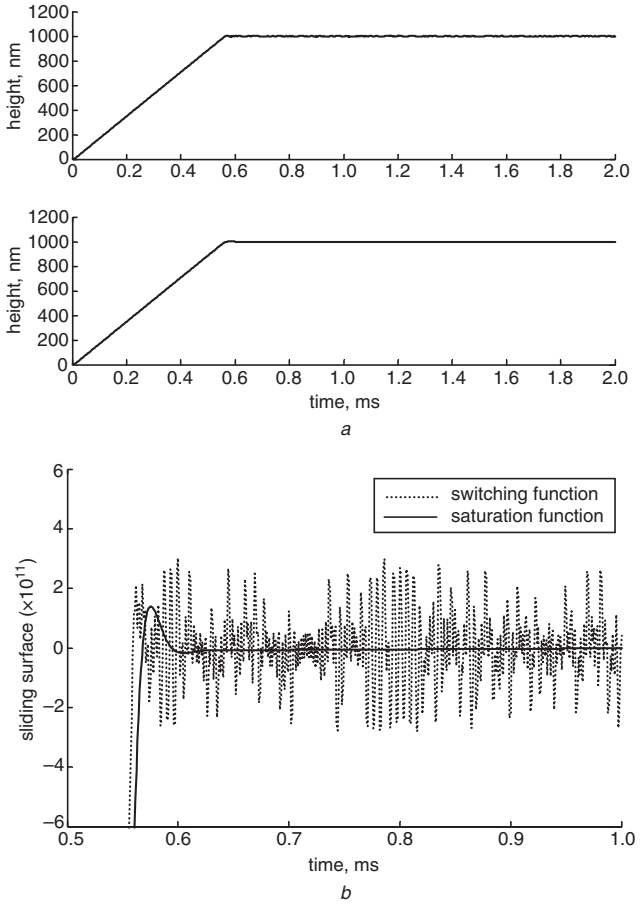

Fig. 5

a Step response of the sliding mode controller with switching function and with saturation function
b Sliding surfaces of the sliding mode controller with switching function and with saturation function

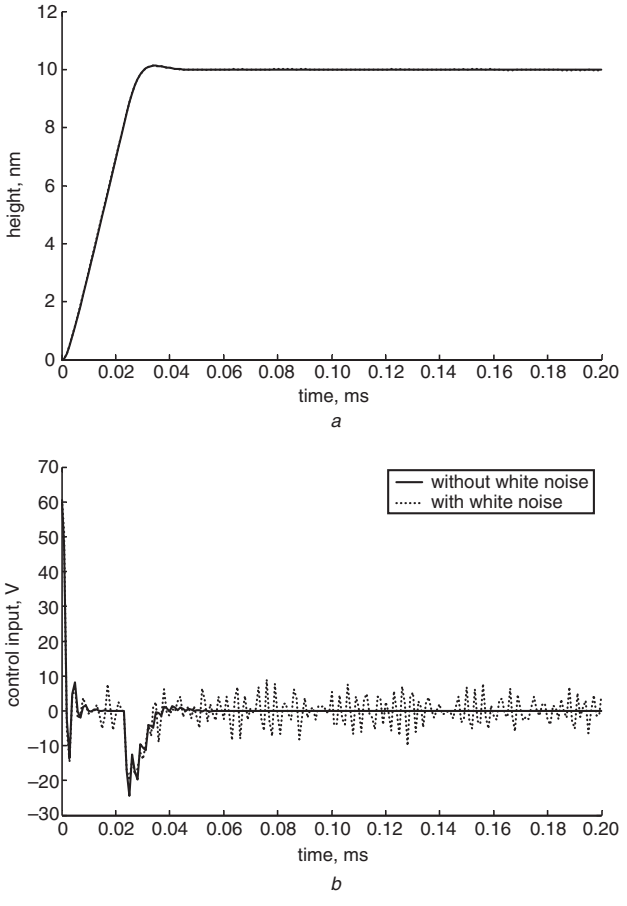

Fig. 6

a Comparison of 10 nm step response with and without white noise disturbance
b Comparison of control inputs with and without white noise disturbance

5.2 Third-order sliding mode control with robust differentiators

The use of robust differentiators i.e. (29) and (30) in the third-order sliding mode controller, (28), leads to the step response and sliding functions, depicted in Fig. 7*a* and Figs. 7*b* to 7*d* respectively. It can be found that the sliding functions, as defined in (20), (22), (23) and (26), indeed converge to zero. The tracking capability does not degrade at all when using robust differentiators for derivative values.

In order to verify the robustness of the present controller with robust differentiators, a white noise is introduced into the measured flying height error signal. The mean and variance of the white noise are 0.0001 and 0.1001, respectively. Figure 8 compares the step responses of the third-order sliding mode controller with and without the robust differentiator. As a result, the controller performances with the presented differentiator does not degrade at all, whereas the other one becomes unstable.

5.3 Fourth-order sliding mode control

Figure 9*a* depicts the step response and Fig. 9*b* the actual control input u created by the modified plant model in (32) and the output feedback fourth-order sliding mode controller of (33). The derivatives of S_0, S_1 and S_2 are directly calculated. The control input in Fig. 9*b* shows that high-order sliding mode control can achieve a smooth control input and reduce chattering.

5.4 Flying height control with measured disk vibration waveform

To validate the proposed controller, we performed a flying height control simulation for the PZT model of (1) using vibration displacement data $v(t)$ of a near-field optical disk. The vibration data is measured by using a dual-beam laser Doppler vibrometer for a polycarbonate-substrate-based near-field optical disk at a constant speed of 5400 rpm. The dominant frequency of the disk vibration is 90 Hz synchronous with the spindle motor speed. The applied PZT bender is model PL122.251 made by Physik Instrumente. Its displacement in the bending direction is 0–250 μm corresponding to an input voltage of 0–60 V.

In order to maintain a constant flying height in the presence of disk vibration, the flying height control can be treated as a trajectory tracking control task dealing with a disk vibration waveform $v(t)$ between approximate ±60 μm, as shown in Fig. 10*a*, so as to control the flying head height equal to the sum of the disk vibration amplitude and a constant flying height h_f, i.e. the focusing depth for a near-field optical disk as depicted in Fig. 1. Hence, the reference input can be expressed as:

$$r(t) = v(t) + h_f \tag{35}$$

Using the third-order sliding mode controller with robust differentiators, the flying height error in tracking the disk

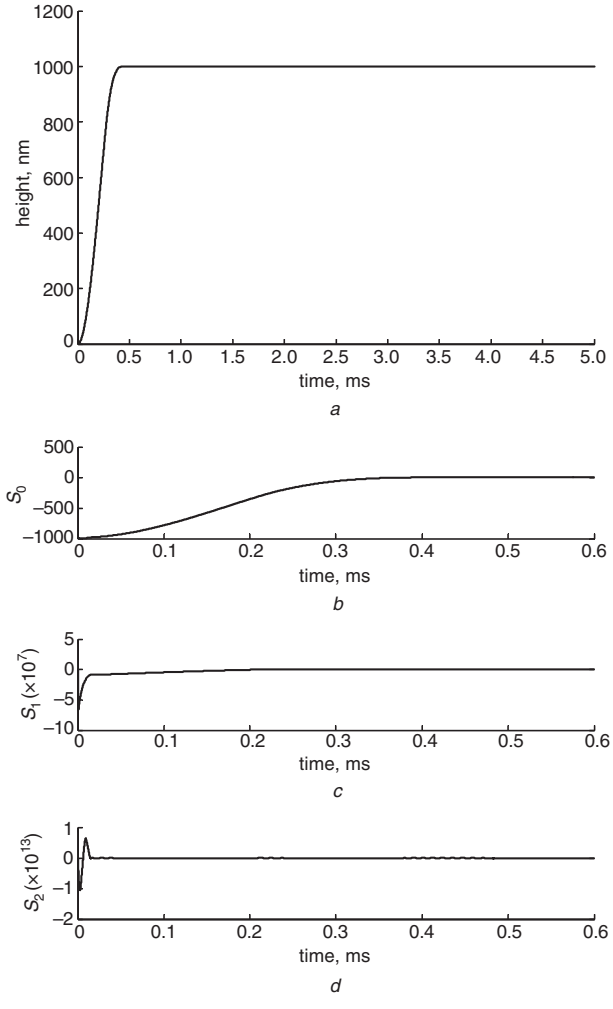

Fig. 7

a Step response of the third-order sliding mode controller with robust differentiators
b Sliding function S_0 of the third-order sliding mode controller with robust differentiators
c Sliding function S_1 of the third-order sliding mode controller with robust differentiators
d Sliding function S_2 of the third-order sliding mode controller with robust differentiators

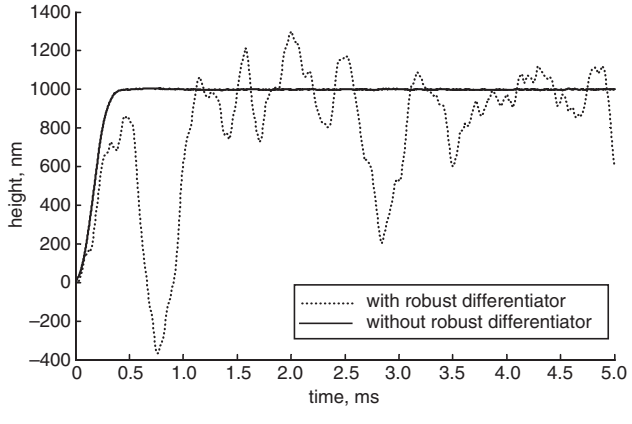

Fig. 8 *Step responses under measurement noise of the third-order sliding mode controller with and without robust differentiators*

vibration waveform is shown in Fig. 10*b*. The tracking control error reduces from the initial value of −242 nm to lie within ±30 nm after 1 ms. The initial large tracking error of up to 93 nm comes from the initial estimation error of the robust differentiator.

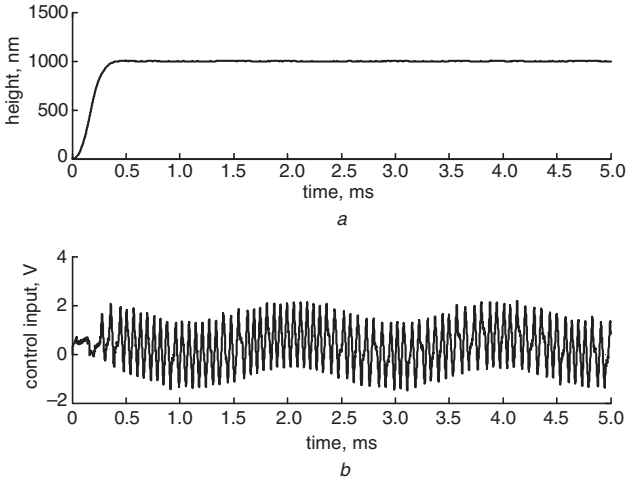

Fig. 9

a Step response of the fourth-order sliding mode controller
b Control input at the fourth-order sliding mode controller

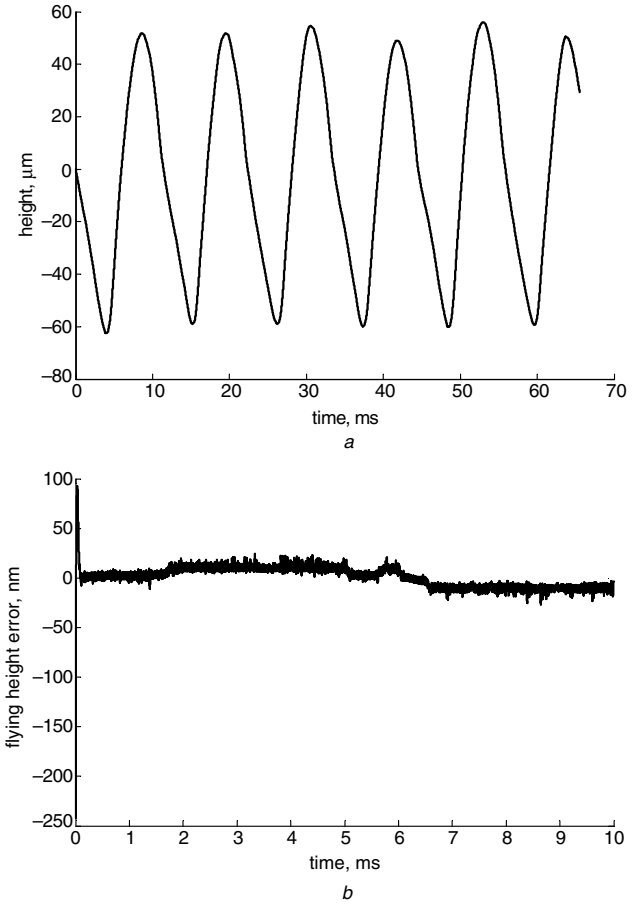

Fig. 10

a Measured surface vibration of optical disk
b Output error in flying height control

6 Conclusions

An output feedback sliding mode flying height controller with a PZT actuator has been developed for flying height control for near-field optical disk drives accompanied by a severe and uncertain disk vibration. In order to reduce the number of required output derivatives and avoid chattering, a high-order sliding mode controller with a robust differentiator has been presented for application in the

flying height control. Simulation results demonstrate the effectiveness of the proposed mechanism and control method.

7 Acknowledgment

This work was supported by 'Photonics science and technology for tera era', Center of Excellence, Ministry of Education, Taiwan under contract 89-E-FA06-1-4.

8 References

1 Milster, T.D.: 'Near-field optics: a new tool for data storage', *Proc. IEEE*, 2000, **88**, (9), pp. 1480–1490
2 Ito, K., Saga, H., Nemoto, H., and Sukeda, H.: 'Advanced recording method using a near-field optics and the GMR head', Optical Data Storage, Conf. Digest, Whistler, Canada, 14-17 May 2000, pp. 30–32
3 Jenkins, D.F.L., Chilumbu, C., Tunstall, G., Clegg, W.W., and Robinson, P.: 'Multi-layer bulk PZT actuators for flying height control in ruggedised hard disk drives', Proc. 12th IEEE Int. Symp. on Applications of ferroelectrics, Piscataway, NJ, USA, 21 July–2 August 2000, vol. 1, pp. 293–296
4 Kobayashi, M., and Horowitz, R.: 'Track seek control for hard disk dual-stage servo systems', *IEEE Trans. Magn.*, 2001, **37**, (2), pp. 949–954
5 Hung, J.Y., Gao, W., and Hung, J.C.: 'Variable structure control: a survey', *IEEE Trans. Ind. Electron.*, 1993, **40**, (1), pp. 2–22
6 Utkin, V.I.: 'Sliding modes in control optimization' (Springer-Verlag, New York, 1993)
7 Levant, A.: 'Universal single-input-single-output (SISO) sliding mode controllers with finite time', *IEEE Trans. Autom. Control*, 2001, **46**, (9), pp. 1447–1451
8 Levant, A.: 'Robust exact differentiation via sliding mode technique', *Automatica*, 1998, **34**, (3), pp. 379–384
9 Yu, X., and Xu, J.X.: 'Variable structure systems: toward the 21st century' (Springer, New York, 2001)
10 Yu, X., and Xu, J.X.: 'Nonlinear derivative estimator', *Electron. Lett.*, 1996, **32**, (16), pp. 1445–1447
11 Dabroom, A., and Khalil, H.K.: 'Numerical differential using high-gain observers'. Proc. IEEE Conf. on Decision and control, San Diego, USA, 10–12 December 1997, pp. 4790–4795
12 Djemai, M., and Barbot, J.P.: 'Smooth manifolds and high order sliding mode control'. Proc. IEEE Conf. on Decision and control, Las Vegas, USA, 10–12 December 2002, pp. 335–339
13 Levant, A., 'High order sliding modes and arbitrary-order exact robust differentiation'. Proc. of European Control conf., 4–7 September 2001, pp. 996–1001